Annales UMCS Informatica AI XII, 2 (2012) 73–85
DOI: 10.2478/v10065-012-0015-1

Annales UMCS
Informatica
Lublin-Polonia
Sectio AI
http://www.annales.umcs.lublin.pl/

A comparison of different modulation techniques performances in an underground multiuser communications scenario

Alina-Mihaela Badescu[1]*

[1] *Dept. of Telecommunications, University POLITEHNICA of Bucharest, bd. Iuliu-Maniu, nr. 1-3, Bucharest, Romania*

Abstract – The potential use of typical commercial communication systems with ultra high frequencies for the underground emergency/military situations will be investigated, as commercial systems have already a fully developed market that makes them cheap and reliable. The possible usage of broadband techniques like CDMA in the direct sequence will be studied because most commercial communication systems have already been designed to support multiple users, as the underground propagation has many possible applications. The performances of both modulation techniques are evaluated from the point of view of the quality of the signals, power spectral density and the effect that the propagation medium has on the transmitted signals such that the best modulation technique is determined. The 16QAM and QPSK modulations (two of the most popular modulation techniques in the terrestrial wireless system) are compared in a scenario where a number of underground sources share the same physical channel (and antenna) - the receiver is placed at the ground level so the generated signals must propagate through the dielectric layer in order to reach it. The transmitted power, electric and magnetic fields as well as occupied bandwidth are also calculated.

1 Introduction

Nowadays underground applications are more and more popular especially due to the technological progress in radio communications. Most applications refer to disaster prevention [**1**], ultra high energy particle detectors [**2**], security and monitoring [**3**] or military use [**4**]. Although very attractive, the challenges involved in this type of applications are major [**5**].

Almost all existing underground systems are based on the line communication principle (wired), hence they are unable to withstand in the disaster conditions as well they

*alinabadescu@radio.pub.ro

are formidable in inaccessible places. Therefore, wireless communication is in indispensable, most reliable, convenient system. It would also help to increase production and productivity in mines.

Wireless underground radio communication has been used so far only with very low frequency part of the spectrum (3k-30kHz). A number of investigations have been carried out for propagation of EM waves through rock with the frequencies up to 60MHz in South America and Africa [**6**]. A subterranean wireless communication system is being developed for wartime for the US Army. It has been tested is the Arizona mines and it can send voice communication through 265m of solid rock and a digital photo through 133m of rock [**5**]. In India, the Instrumentation Division of Central Mining Research Institute, Dhanbad, is actively engaged in development of various wireless communication systems for different locations in the underground mines [**7**].

The existing systems for underground communications are slow and inefficient because the higher noise levels (associated with low frequency transmission) and lower signal levels necessitate the incorporation of nonlinear processing and adaptive noise cancellation –and the necessary demodulation processing [**8**]. This prompted the development of wireless electromagnetic systems based on seismic or electromagnetic methods. The electromagnetic narrowband method is a highly expensive one as it involves design and development of circuits and systems (such as the high-temperature Superconducting Quantum Interference Devices system, developed for DOE [**9**]), which are essential for the underground mines and hazardous areas. More to that, low-frequency receivers are relatively insensitive to low frequency magnetic fields when configured into small packages and used over a wide bandwidth. Progress in the wide bandwidth underground communications has already started to show with development of antennas designed for this type of communications [**10**].

Underground mines, which are characterized by their tough working conditions and hazardous environments, require fool-proof wide communication systems for smooth functioning. A reliable and effective communication system is also an essential requisite for safety. This is the reason why we will investigate the potential use of typical commercial communications systems with the ultra high frequencies (300MHz-3GHz) for the underground emergency/military situations. The commercial systems have a fully developed market that makes them cheap and reliable. As underground propagation has many possible applications, we will study the possible usage of broadband techniques like multiple access with code division in a direct sequence because most commercial communication systems have already been designed to support multiple users.

The second purpose of the paper is to determine the best modulation technique for such a scenario. We will evaluate its performances from the point of view of the quality of the signals, power spectral density and the effect that the propagation medium has on the transmitted signals.

We decided to compare the 16QAM and QPSK modulations (two of the most popular modulation techniques in the terrestrial wireless system) in a scenario where a number

of underground sources share the same physical channel (and antenna). Here the sources are buried completely in a salt mine. The receiver is placed at the ground level so the generated signals must propagate through the dielectric layer in order to reach it. We have also calculated the transmitted power, electric and magnetic fields and occupied bandwidth.

This article is structured as follows: in Section II we will present briefly the mathematical models for both modulation and propagation. Section III is dedicated to the numerical results we have obtained. The last section presents our main conclusions.

2 Mathematical Model

We will first present the model of the communication system with multiple access and code division in the direct sequence, applied on the period of a bit transmission from each user. Data transmission is synchronous, in the sense that the transmission rate and the moment of emission are the same for all users.

The common channel is shared by four users, each associated with a spread code sequence $s_k(t)$. The noise-less signal will be [**11**]:

$$y_{ss}(t) = \sum_{k=1}^{N} V_k b_k s_k(t), \quad t \in [0, T_b] \tag{1}$$

where T_b is the bit period, $b_k \in \{-1, 1\}$ represents the bit emitted by the user k in the period T, V_k is the amplitude of the user k. The code sequences are normed so that the energy is set to the unit for each user:

$$\int_0^T s_k^2(t)dt = 1. \tag{2}$$

As the step function $y_{ss}(t)$ has q different amplitudes A_i, $i = 1, \ldots, q$, in order to modulate it, we will write it as a sum of digital signals $y_i(t)$. Each signal has a single amplitude A_i:

$$y_{ss}(t) = \sum_i A_i y_i(t). \tag{3}$$

Each of the i^{th} signals will be modulated first using a QPSK modulation and after with a 16QAM modulation. As both are quadrature modulations, the general form of each signal can be written as:

$$y_i(t) = Q_1(nT_b)\sin(\omega t) + Q_2(nT_b)\cos(\omega t) \tag{4}$$

where T_b is the bit period, n is a positive integer ($n = 1, \ldots, N$), ω is the pulsation corresponding to the carrier frequency and $Q_{1,2}$ are two–step functions with different amplitudes according to the modulation type and transmitted bits.

The modulated signals will be transmitted using an ideal transmitting dipole of length l (its geometry in the spherical coordinate is given in Fig. 1). As both modulations are quadrature, we will write the generated electric and magnetic fields in a unified parameterization using the terms C and S that are two functions of time, transmitted bit, modulation type and amplitude. The S factor also includes a multiplying factor of $\exp(j\pi/2)$, given by the slightly different current distribution on the antenna, obtained from the sine compared to the cosine factor in (4). In this way, the fields can be expressed in the spherical coordinate system (r, θ, ϕ) with the unit vectors a_r, a_ϕ and a_θ:

$$\vec{E} = \frac{-\cos\theta\lfloor jv_g - \omega r - j\cos(kl)v_g + \cos(kl)\omega(kl)\omega r\rfloor \exp(-jkr)(C-S)}{\pi\varepsilon_0 r^3 \omega k v_g}\vec{a_r} - \frac{-0.5\sin\theta(jv_g^2 - r\omega v_g - \omega^2 r^2 - j\cos(kl)v_g^2 + \cos(kl)r\omega v_g + \cos(kl)r^2\omega^2)}{\pi\varepsilon_0 r^3 \omega k v_g^2} \cdot \exp(-jkr)(C-S)\vec{a_\theta} \quad (5)$$

$$\vec{H} = \frac{\sin\theta(-v_g - \omega d + \cos(kl)\omega r)\exp(-jkr)(C-S)}{2\pi r^2 k v_g}\vec{a_\phi} \quad (6)$$

where ε_0 is the electric permittivity of vacuum, ε_r is the relative permittivity of the medium, j is the complex number, ν_g is the group velocity in the propagating medium (we have considered only homogeneous, non-dispersive dielectric media with the relative permeability ß$_r = 1$, thus $\nu_g = c/\sqrt{\varepsilon_r}$) and is the wave vector. Each wave is completely described by the electric field, the magnetic one and the wave vector. The wave vector modulus is:

$$k\frac{\omega\sqrt{\varepsilon_r}}{c}. \quad (7)$$

Note that k is a real number if $\sqrt{\varepsilon_r}$ is real and it becomes complex when the wave is propagating in the lossy medium with $\varepsilon_r = \Re\{\varepsilon_r\} + j\Im\{\varepsilon_r\}$. For a dielectric the imaginary part is a measure of the loss. Its sign should be chosen in such a way that $\Im\{k\} > 0$ as the wave is dumped in the dielectric. Another way of describing losses is by the loss tangent defined as the radio of real to imaginary part of the permittivity. In this paper scattering effects will be neglected as the impurities in the medium have usually small sizes compared with the radio wavelength of radiation.

The instantaneous radiated power at any point P (in Fig. 1) is given by:

$$P(t) = \frac{1}{2}\Re\left\{\int_\theta\int_\phi \vec{E}\times\vec{H}^* d\vec{A}\right\} \quad (8)$$

where $d\vec{A}$ is the unit area and $\vec{H}$ is the complex conjugate of the magnetic field. The total generated power throughout the transmission is:

$$P_{med} = \frac{1}{2T}\Re\left\{\int_t\left(\int_\theta\int_\phi \vec{E}\times\vec{H}^* d\vec{A}\right)dt\right\}. \quad (9)$$

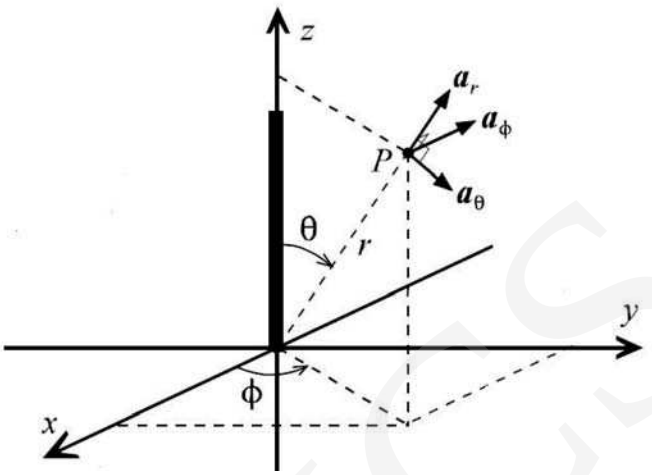

Fig. 1. A dipole of length l in the spherical coordinate. The unit vectors are a_r, a_ϕ and a_θ.

3 Numerical results

In the following we will consider a situation when four users transmit each $N_b = 10$ bits. They all use the same power so the amplitude vector in eq. (1) is $V = \begin{bmatrix} 4 & 4 & 4 & 4 \end{bmatrix}$. The spread code sequences, of length 8, are:

$$s_1 = \begin{bmatrix} 1 & 1 & 1 & -1 & 1 & 1 & 1 & -1 \end{bmatrix} / \sqrt{8};$$
$$s_2 = \begin{bmatrix} 1 & 1 & 1 & -1 & -1 & -1 & -1 & 1 \end{bmatrix} / \sqrt{8};$$
$$s_3 = \begin{bmatrix} 1 & 1 & -1 & 1 & 1 & 1 & -1 & 1 \end{bmatrix} / \sqrt{8};$$
$$s_4 = \begin{bmatrix} 1 & 1 & -1 & 1 & -1 & -1 & 1 & -1 \end{bmatrix} / \sqrt{8}.$$

The $\sqrt{8}$ factor assures the unit energy condition (2).

Using eq. (1) we can calculate the digital signal $y_{ss}(t)$ - presented at the bottom of Fig. 2. As its amplitude has four different values (± 2.8284 and ± 5.6569), we will write it as a sum of four digital signals of amplitudes $\pm A_m = \pm 2.8284$ and $\pm A_{mM} = \pm 5.6569$. In this way, similar to eq. (3):

$$y_{ss}(t) = A_m y_a(t) - A_m y_b(t) - A_{mM} y_c(t) + A_{mM} y_d(t). \tag{10}$$

Each of the four signals $y_{a/b/c/d}(t)$ will be modulated first using the QPSK technique (denoted from now on with the index QPSK) and after using a 16QAM modulation (denoted with the index QAM). In both cases the carrier frequency is set to 800MHz. The bit period is set to $T_b = 10^{-6}$s.

For the QPSK modulation, each signal will be computed as:

$$y_{i,QPSK}(t) = b_{i,o}(t) \cos(\omega t) - b_{i,e}(t) \sin(\omega t), \qquad i \in \{a, b, c, d\} \tag{11}$$

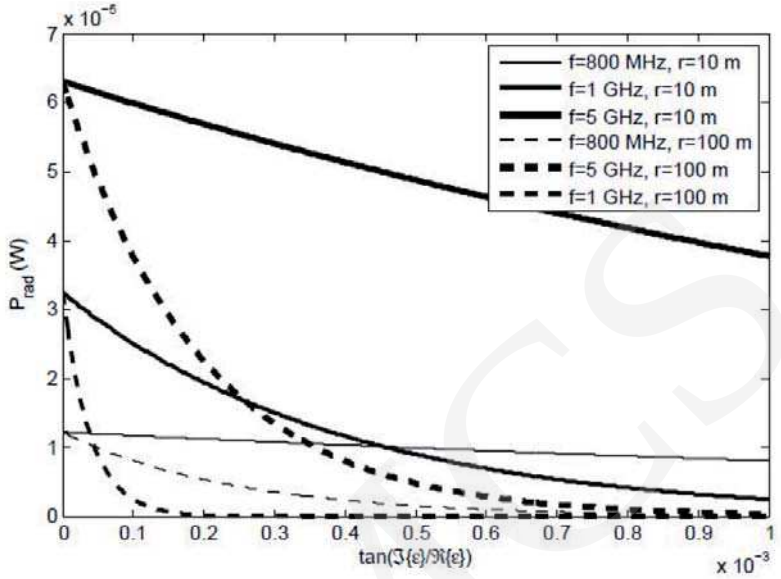

Fig. 2. The power expressed in terms of the tangent loss. We have considered the frequencies of 800 MHz (thin lines), 1 GHz (thicker lines) and 5 GHz (thickest lines) and computed the received power at $r = 10$m (solid lines) and $r = 100$m (dashed lines). We have considered $\Re\{\varepsilon_r\} = 6$.

where $b_{o/e}$ represents the odd/even bit stream of the i^{th} signal. Note that as $b_{o/a\in\{0,1\}}$, a conversion from this interval to $\{-1, 1\}$ must be made. The transmitted signal $y_{ss,QPSK}(t)$ will be calculated as:

$$y_{ss,QPSK}(t) = y_{a,QPSK}(t) + y_{b,QPSK}(t) + y_{c,QPSK}(t) + y_{d,QSPK}(t). \tag{12}$$

Due to the sign of the amplitudes (equal in modulus two by two but opposite as sign), the total transmitted signal shows a zero value between [3.91,6.81]T_b, [11.93, 13.83] T_b, [14.84, 15.94]T_b, [27.97, 29.87]T_b, [30.98, 31.88]T_b, [36, 37.99]T_b, [39, 40]T_b which can lead to large errors at demodulation. This problem associated with an optimal spread code sequence will be addressed in a future paper.

For the 16QAM modulation, each signal will be computed as:

$$\begin{aligned} y_{a/b/c/d,QAM}(t) = {} & \lfloor P_1 b_{i,4k+1}(t) + P_2 b_{i,4k+2}(t) \rfloor \cos(\omega t) \\ & - \lfloor P_2 b_{i,4k+3}(t) + P_1 b_{i,4k}(t) \rfloor \sin(\omega t), \quad i \in \{a, b, c, d\} \end{aligned} \tag{13}$$

where the amplitudes are $P_1 = 2V$ and $P_2 = 1V$; $b_{i,4k+g}$, $g = 0, \ldots, 3$ represents the bit number of the i^{th} signal. Again a conversion to $\{-1, 1\}$ interval must be made. The transmitted signal $y_{ss,QAM}(t)$ can be calculated as:

$$y_{ss,QAM}(t) = y_{a,QAM}(t) + y_{b,QAM}(t) + y_{c,QAM}(t) + y_{d,QAM}(t). \tag{14}$$

The transmitted signal shows a zero value between $[3.92, 5.82]T_b$ and $[11.96, 12.96]T_b$. Compared with the QPSK case when the signal was equal to zero 29.22% of time, the 16QAM case shows improvement, being zero only 14.5% of time.

For the QPSK and 16QAM signals we have calculated their spectra. For the QPSK signal, the occupied bandwidth is equal to 39.216 MHz. For the 16QAM the bandwidth is 30% lower, that is 27.451 MHz. These properties are summarized in Table 1.

Table 1. Comparison of properties of signals.

	%time when equal to zero	Bandwidth [MHz]
QPSK signal	29.22	39.21
16QAM signal	14.5	27.45

So far we have presented only the modulation technique. The signals that are emitted deep underground must propagate towards the surface by crossing different environments. We will investigate only the far field problem because in this paper we have considered characteristics of a typical Romanian salt mine, 'Unirea', in Slanic Prahova, situated at 208 m below the surface (thus $r \gg l$).

For the sake of comparison, we have simulated the situation when an ideal dipole antenna emits directly in a dielectric medium a simple cosine waveform of amplitude 1A. From here on, we have always considered the case of a dipole of the length $l = 80$cm. This length has been chosen as it represents a typical commercial cheap antenna.

The power can be calculated with (8) and for an ideal medium (with no loss) is independent of the distance r. For propagation in air, the power is 0.5067W and for propagation in pure salt ($\Re\{\varepsilon_r\} = 6$), it is $0.1223 \cdot 10^{-4}$W. We have chosen this value of the permittivity because the studies have shown that salt has a dielectric constant in the 5-7 range and a tangent loss of 0.015 to 0.030 at 300 MHz [**12**].

For a lossy medium, the power depends on the tangent loss – $\tan(\delta) = \tan(\Im\{\varepsilon_r\}/\Re\{\varepsilon_r\})$ – and becomes dependent on the distance that waves travel. In Figure 2 we have considered the case of propagation in impure salt. It can be easily observed that the power with all considered frequencies decreases with the distance and with the increase in the imaginary part of the permittivity.

We will move on to the modulated signals (eqs. (11) and (12)) and present the total electric and magnetic fields. For propagation in air, at a carrier frequency of 800MHz, the fields have been simulated as the function of r and θ.

For a given value of θ (here $\theta = 30^0$), it can be clearly seen in Figs. 3 and 4 that the electric and magnetic fields decrease with the value of r for both modulation types. For the QPSK, the temporal variations within a bit period are extremely fast which requires an expensive receiver with fast commutation circuits. The synchronization will also represent a problem at demodulation.

The 16QAM signal has more amplitude levels than QPSK. The sinusoidal behaviour of fields (Figure 4) will make even harder the signal recovery at demodulation as very

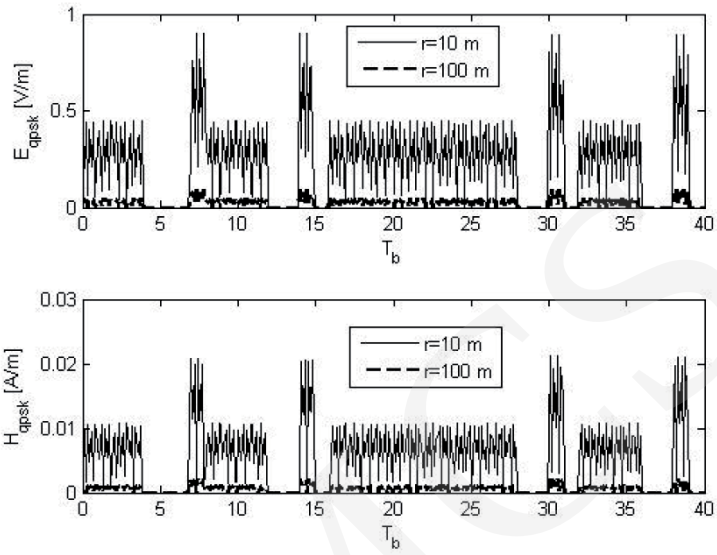

Fig. 3. Electric (top) and magnetic (bottom) fields for the QPSK modulated signal at $r = 10$m (continuous line) and at $r = 100$m (dashed line) when $\theta = 30^0$.

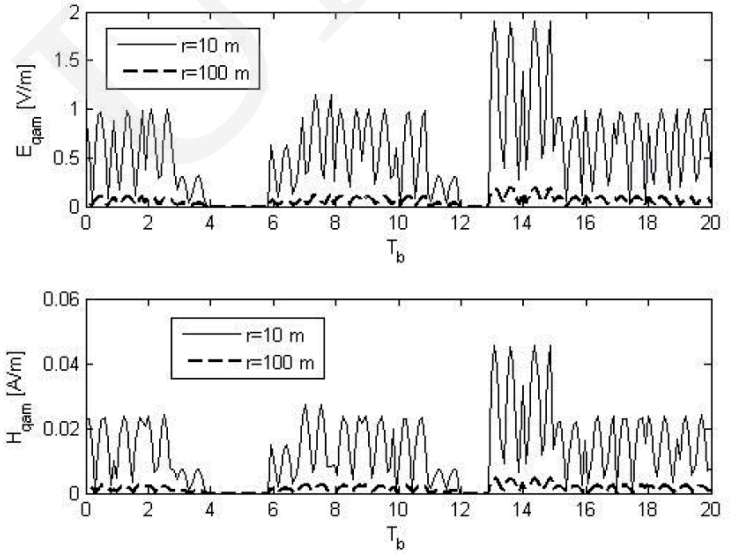

Fig. 4. Electric (top) and magnetic (bottom) fields for the 16QAM modulated signal at $r = 10$m (continuous line) and at $r = 100$m (dashed line) when $\theta = 30^0$.

close decision thresholds must be used to estimate the transmitted bits. The advantage is that time variation within the bit period is smaller thus less expensive receivers are required.

The same observations about the time variation and decision intervals can be made from the simulations on the variation of fields with the angle (at constant r). Their magnitude gets higher as θ approaches 90^0 for both modulation types.

The instantaneous radiated power as the function of the bit period is represented in Fig. 5. We have consideredpropagation in both a dielectric without losses ($\varepsilon_r = 6$) and in a typical salt dome where the permittivity of the medium is around $\varepsilon_r = 6+j10^{-3}$. In the case of propagation in lossless medium, the power (eq. (8)) is independent of θ and r. In the case of propagation in lossy dielectrics, the power becomes dependent on the distance at which it is calculated (in Fig. 5 we have calculated it with $r = 100$m). One can observe that losses in the dielectric produce decrease in power. The higher power levels are more affected in understand as the absolute value. The QPSK modulation shows power one order of magnitude smaller than 16QAM.

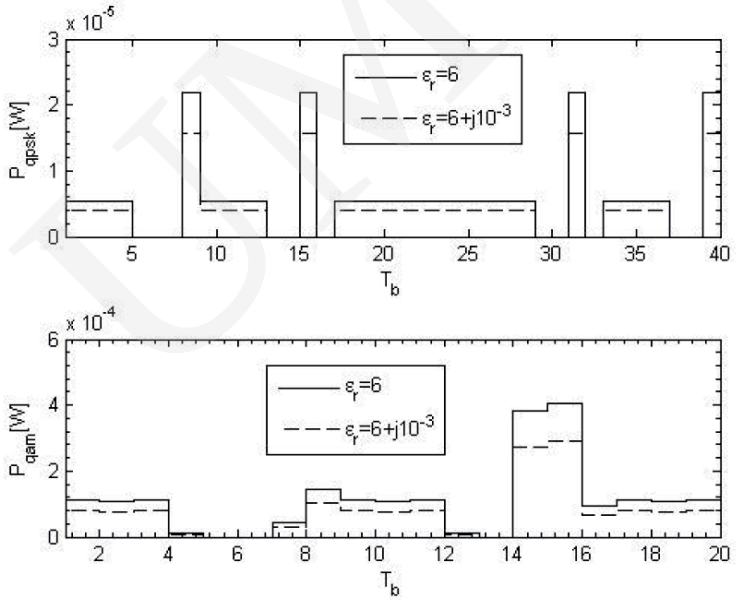

Fig. 5. Power of the QPSK (top) and 16QAM (bottom) signals as the function of the bit period for a lossless dielectric with $\varepsilon_r = 6$ (continuous line) and in dielectric with $\varepsilon_r = 6 + j10^{-3}$ (dashed line) for which we considered propagation at $r = 100$m.

We will determine next the influence of the absorptions in the medium on the total power (eq. (9)) by varying the imaginary part of the permittivity. Its real part has been chosen to be constant and equal to six. Propagation in the lossy media is strongly affected by the distance covered by the waves, thus it is expected for the power to

decrease with r. Figure 6 presents the total radiated power at three distances (50m, 200m and 400m) as the function of $\Im\{\varepsilon_r\}$. One can observe the influence of r as predicted. For very small losses (less than 10^{-4}) the power does not show strong dependence on the distance. Again the power of the 16QAM signal is one order or magnitude higher than in the case of QPSK. The power has an overall tendency to decrease with the increase of $\Im\{\varepsilon_r\}$. The sinusoidal behaviour comes from the $\cos(kl)$ factor in eqs. (6) and (7).

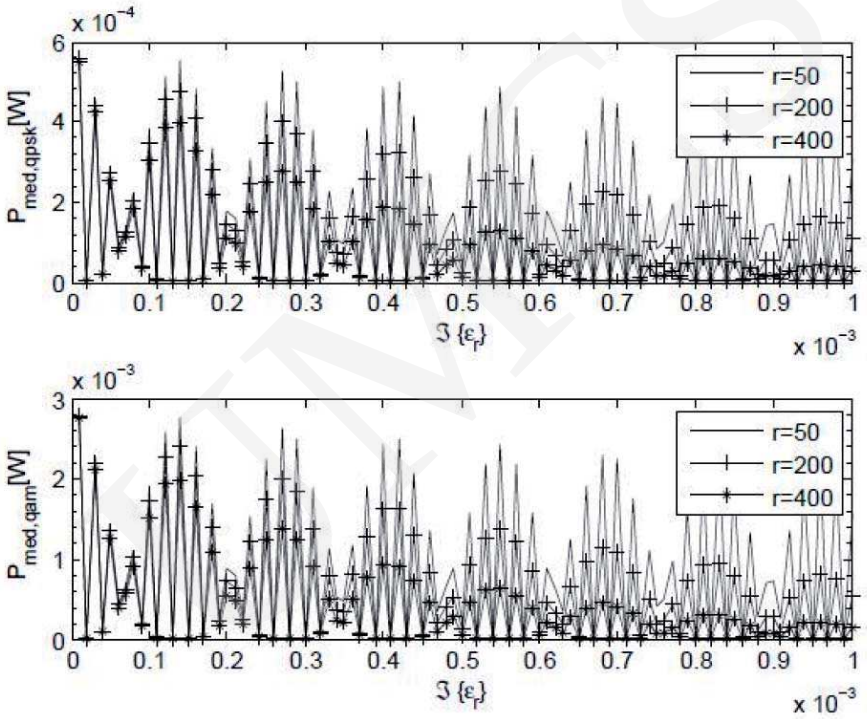

Fig. 6. Total power of the QPSK (top) and 16QAM (bottom) signals as the function of the imaginary part of the permittivity calculated at $r = 50$m (dotted line), $r = 200$m (line marked with '+') and at $r = 400$m (line marked with '*'). We considered $\Re\{\varepsilon_r\} = 6$.

The improvement in power level introduced by the quadrature modulations can be clearly seen by comparing the un-modulated signal in Fig. 2 and the modulated signals in Fig. 6. The QPSK modulation increases the power 10 times while the 16QAM -100times.

The influence of the distance covered by the waves in a lossy dielectric can be seen in Fig. 7. We have considered $\varepsilon_r = 6 + j10^{-3}$ and calculated the instantaneous power when the signals covered the distance of 100, 200 and 300m. As expected, the power drops.

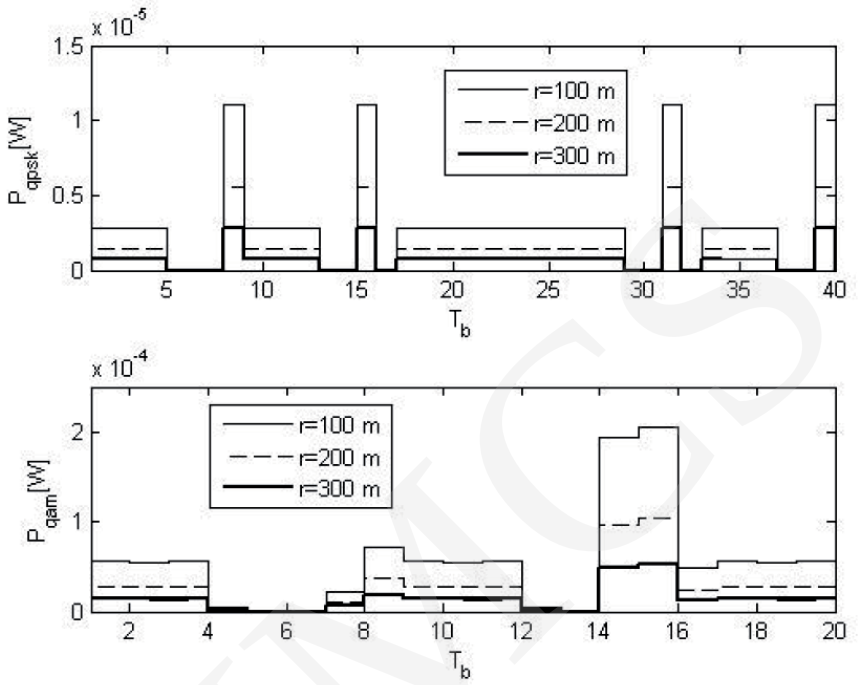

Fig. 7. Power of the QPSK (top) and 16QAM (bottom) signals as the function of the bit period for a dielectric with $\varepsilon_r = 6 + j10^{-3}$ calculated at $d = 100$m (continuous, thin line), $d = 200$m (dashed line) and at $d = 300$m (continuous, thick line).

The most affected signal is the 16QAM one as the differences in the power levels are not longer visible for propagation in over 200 m of lossy dielectric. This can lead to large errors at demodulation and signal recovery may not even be possible anymore.

4 Conclusions

As the existing systems for the underground communications at VLF are slow and inefficient, we investigated the possibility of using the typical commercial communication techniques at UHF with a developed and mature market.

We compared the 16QAM and QPSK modulations in a scenario where a number of underground sources shared the same physical channel (and antenna). The receiver was placed at the ground level so the generated signals had to propagate through the dielectric layer in order to reach it. We calculated the transmitted power, electric and magnetic fields and occupied bandwidth for both modulations. We have evaluated their performances from the point of view of the quality of the signals, power spectral density and the effect that the propagation medium has on the transmitted signals.

The first observation we made is that the used spread code sequence can give rise to large errors at demodulation because the total transmitted signal can be zero. From this point of view, the QPSK signal is more vulnerable. For this reason, optimization of codes will be addressed in a future article.

The occupied bandwidth of 16QAM signal is 30% smaller than in the case of QPSK and this is another key point in favour of the 16QAM transmission.

When compared to an un-modulated signal, the improvement introduced by the quadrature modulations in the power level is evident (for the QPSK modulation it is 10 times better while for the 16QAM, 100 times).

If one is interested in measuring the electromagnetic fields generated, QPSK techniques require fast commutation circuits and precise synchronization for measurements. This is not a problem for the 16QAM technique that instead requires more data processing thus more memory and more performant CPU. For the receiving system, 16QAM is associated with a higher sensitivity in amplitude while the QPSK with a very good time resolution.

The height of the absorbing dielectric is one crucial factor and we have demonstrated that propagation of 16QAM signals in over 200m of lossy dielectric (salt, in our case) is making data recovery impossible from the power measurements. Compared to 16QAM signal, the QPSK is showing a power one order of magnitude smaller.

We conclude that the typical commercial communication techniques can be successfully used. For propagation at the distances larger than 200m, the modulation must be QPSK. For propagation at the distances smaller than 200m, 16QAM signals have overall performances better than QPSK.

References

[1] Mo L., Yunhao L., Underground coal mine monitoring with wireless sensor networks, ACM Transactions on Sensor Networks (TOSN) (2009): 5.

[2] Connolly A., Goodhue A., Miki C., Nichol R., Saltzberg D., Measurements of radio propagation in rock salt for the detection of high-energy neutrinos, Nuclear Instruments and Methods in Physics Research A 599 (2009): 184.

[3] Akyildiz I. F., Stuntebeck E. P., Wireless underground sensor networks: Research challenges, Ad Hoc Networks 4 (2006): 669.

[4] Sterling C., Military Communications: From Ancient Times to the 21st Century, ABC-CLIO: USA (2008).

[5] Mognaschi E. R., On the possible origin, propagation and detectability of electromagnetic precursors of earthquakes, Atti Ticinensi di Scienze della Terra 43 (2002): 111.

[6] Bandyopadhyay L. K., Chaulya S. K., Mishra P. K., Wireless Communication in Underground Mines - RFID-based Sensor Networking, Springer-Verlag: New York (2009).

[7] Bandyopadhyay L. K., Mishra P. K., Kumar S., Narayan A., Radio frequency communications systems in underground mines; http://www.wvminesafety.org/PDFs/communications/Additional%20Documents/Communication _Systems_in_Underground_Mines.pdf (20.06.2011).

[8] Raab F. H., Signal processing for through-the-earth electromagnetic systems, IEEE Transactions on Industry Applications 24 (1988).

[9] Geophysical Technologies for Detecting Underground Coal Mine Voids, July 28-30, 2003, Lexington, Overview of Mining Industry of the Future; http://www.fhwa.dot.gov/engineering/geotech/hazards/mine/workshops/ktwkshp/ky0302.pdf

[10] Nedil M., Denidni T. A., Djaiz A., Habib A. M., A new ultra-wideband beamforming for wireless communications in underground mines, Progress In Electromagnetics Research M 4 (2008): 1.

[11] Halunga S., Fratu O., Vizireanu D., Telecommunications systems with CDMA, ETF: Bucharest (2000).

[12] Annan A., Davis J. L., Gendzwill D., Radar sounding in potash mines, Saskatchewan, Canada. Geophysics (1988).